Successes and failures of Hubbard-corrected density functional theory: The case of Mg doped $LiCoO_2$

Juan A. Santana,[1] Jeongnim Kim,[1] P. R. C. Kent,[2,3] and Fernando A. Reboredo[1, a)]
[1)] *Materials Science and Technology Division, Oak Ridge National Laboratory, Oak Ridge, TN 37831, USA*
[2)] *Center for Nanophase Materials Sciences, Oak Ridge National Laboratory, Oak Ridge, TN 37831, USA*
[3)] *Computer Science and Mathematics Division, Oak Ridge National Laboratory, Oak Ridge, TN 37831, USA*

(Dated: 7 November 2014)

We have evaluated the successes and failures of the Hubbard-corrected density functional theory (DFT+U) approach to study Mg doping of $LiCoO_2$. We computed the effect of the U parameter on the energetic, geometric and electronic properties of two possible doping mechanisms: (1) substitution of Mg onto a Co (or Li) site with an associated impurity state and, (2) formation of impurity-state-free complexes of substitutional Mg and point defects in $LiCoO_2$. We find that formation of impurity states results in changes on the valency of Co in $LiCoO_2$. Variation of the Co U shifts the energy of the impurity state, resulting in energetic, geometric and electronic properties that depend significantly on the specific value of U. In contrast, the properties of the impurity-state-free complexes are insensitive to U. These results identify reasons for the strong dependence on the doping properties on the chosen value of U and for the overall difficulty of achieving agreement with the experimentally known energetic and electronic properties of doped transition metal oxides such as $LiCoO_2$.

arXiv:1406.3053v2 [cond-mat.mtrl-sci] 6 Nov 2014

I. INTRODUCTION

Although theory has been used to support research in new rechargeable battery materials,[1] whether theory can be used to design new materials without experimental input will largely depend on the ability of electronic structure methods to describe new and existing materials with accuracies compatible with experimental needs.[2–4] Thus, in order to respond to initiatives such as the Materials Genome,[5] the predictive power of theory must be characterized.

In energy storage research, a significant challenge is to accurately predict the thermodynamic phase stability and ionic/electronic conductivity of cathode materials.[1,6–8] This is because theoretical calculations are mainly based on Density Functional Theory (DFT) within the local density (LDA) and generalized gradient (GGA) approximations. While these approximations are accurate enough to study the thermodynamic and conductive properties of many materials, they are unreliable in others, e.g., transition metal-oxides. Approximations such as LDA and GGA do not account properly for exchange and correlation effects in transition metal-oxides, leading to exchange-correlation errors such as the self-interaction error.[9] In practice a semi-empirical approach is adopted in an attempt to minimize these errors, but the use of experimental data for the calibration and validation inevitably reduces the predictive power of the method.

The doping of cathode materials is an example where it is crucial to accurately predict thermodynamic and conductive properties and where a predictive theory is highly desired. A case that exemplifies the problem is the doping of $LiCoO_2$ with cations such as Mg. The effect of Mg-doping on the electronic conductivity and long-term capacity retention of layered $LiCoO_2$-based batteries have been extensively studied.[10–33] Carewska *et al.*[10] and Tukamoto and West[11] showed that doping $LiCoO_2$ with Mg increases its electronic conductivity. This higher conductivity was rationalized by considering the generation of electronic holes due to the formation of a mixed +3/+4 valence state in Co.[10,11] Later studies[17,18,34–36] supported this model and suggested that the transfer of an electron from Co ion to O $2p$ hole is also involved in raising the conductivity. The formation of oxygen vacancies in Mg-doped $LiCoO_2$ has also been proposed to contribute to the higher conductivity.[15,16,30]

In addition to the increased conductivity, a significant capacity retention for Mg-doped $LiNiCoO_2$-based batteries was independently reported by Chang *et al.*,[37] Cho[38] and Kweon *et al.*[39] For example, Cho found 92% capacity retention for $LiNi_{0.74}Co_{0.22}Mg_{0.04}O_2$ after 94 cycles at 1 C rate vs. 70% for $LiNi_{0.74}Co_{0.26}O_2$.[38] Mg-doping also improves the thermal stability of Li-ion batteries. Similar improved capacity and thermal properties were later reported by other authors for $LiCoO_2$-based batteries.[12–15,17–33] However, doping $LiCoO_2$ and $LiNiO_2$ based cathode materials with Mg cations has the drawback of decreasing the capacity[11,13,37–39] because Mg reduces the concentration of the active Ni^{3+} or Co^{3+} ion sites.[11,37,38]

Several explanations for the stability of Mg-doped Li-ion batteries have been proposed. Cho proposed that a lower cation mixing in $LiNi_{0.74}Co_{0.26-x}Mg_xO_2$ than in $LiNi_{0.74}Co_{0.26}O_2$ battery leads to the improved stability.[38] A large degree of cation mixing, where Li ions

[a)] Electronic mail: reboredofa@ornl.gov

partially occupy the Ni (Co) sites and vise versa, results in lower capacity and affects the structural stability of the layered material.[38,40]

The higher stability has also been rationalized as a pillaring effect, where Mg located in the oxide layers or inter-layer spaces prevents the structural collapse and crystallinity loss during charge/discharge. However, it is still unclear if Mg is located in oxide layers or inter-layers spaces, i.e. whether Mg is on Li or transition metal sites. It has been proposed that Mg is initially on the transition metal sites, but it migrates to the inter-layer spaces after initial cycling.[22,41–43] Xiang *et al.*[44] proposed a similar model based on a detailed analysis of measured change in the volume of $LiNi_{0.80-x}Co_{0.20}Mg_xO_2$ as function of x and possible substitutions and charge balance mechanisms for Mg. They suggested that the stronger Mg-O bond (vs. Li-O) enhances the stability of $LiNi_{1-x}Co_xO_2$-based batteries. On the other hand, Chang *et al.*[37] found that Mg cations are mainly on Ni sites. They argued that Mg stabilizes the NiO_2 slab, preventing thermal and cycling decomposition.[37] Tatsumi *et al.*[45] also found Mg cations to preferentially replace Ni sites initially, but to diffuse out of the active material during cycling. More recently, Tavakoli *et al.*[46] proposed that a short-range ordering of Ni cations around Mg results on $LiNi_{0.755}Co_{0.147}Al_{0.045}Mg_{0.053}O_2$ batteries 34.2 $\pm$ 9.3 meV more thermodynamically stable than undoped $LiNi_{0.800}Co_{0.155}Al_{0.045}O_2$. Such stabilization can provide stronger bonding and prevent the formation of NiO-like phase during charge/discharge.[46]

Despite the significant experimental efforts outlined above, it is still unclear how Mg-doping improves the stability of $LiCoO_2$ and $LiNiO_2$ based batteries. In part, this is because no theoretical work has been performed to evaluate the thermodynamic profile of Mg in these batteries. Calculations have mainly focused on the electronic properties,[18,34,35] lattice stability[36] and Li-intercalation voltage[36] of Mg-doped $LiCoO_2$. Calculations have also been employed to study the site preference of Mg in $LiNiO_2$ by combining theory, x-ray absorption near-edge structure and electron energy-loss near-edge structure measurements.[45]

The relative lack of calculations for the thermodynamics of Mg in these cathode materials comes because such calculations of impurities in transition metal-oxides are rather difficult within the framework of DFT. This is mainly because of DFT errors in transition metal-oxides. These errors can be partially removed by introducing an on-site Hubbard model correction (DFT+U).[47] This method has been successfully used to study Li-ion battery cathodes,[45,48–51] and other transition metal-oxides.[52–54] It is also the standard approach adopted by the "Materials Project"[54] for high throughput computation of materials, including metal-oxides. However, physically, the parameter U should depend on the chemical environment of the atomic site where it is applied, while in conventional DFT+U calculations a universal value of U is used. As a result DFT+U often fails to correctly predict the relative energy between systems with a mixture of localized and delocalized electronic states.[53] This is particularly problematic if one uses DFT+U to study dopants that can induce localized or delocalized states in transition metal-oxides.

Mg is a divalent dopant and its substitution onto a Co or Li site can induce a localized or delocalized state in $LiCoO_2$. Therefore, to elucidate how Mg improves the performance of the $LiCoO_2$ cathode material using DFT/DFT+U methods, a first step is to study how sensitive the calculated properties of Mg-doped $LiCoO_2$ are to different choices of the parameter U. To this end, we studied the effect of U on the energetic, geometric and electronic properties of Mg when it is located on Co and Li sites as well as when it forms complexes with Li vacancies or interstitial sites in $LiCoO_2$.

The remainder of this article is organized as follows. We first discuss the doping mechanisms that were examined, the computational methods employed and how the chemical potentials were established. We then present our results. We start by analyzing the effect of the U parameter on the range of chemical potentials, emphasizing the effect on the phase boundaries of $LiCoO_2$. Subsequently, we discuss the effect of U on the formation energy, geometry and electronic structure of Mg-doped $LiCoO_2$. We conclude with a summary and our conclusions.

II. METHODOLOGY

A. Substitutional Mg in $LiCoO_2$

Mg is formally a divalent dopant, Mg^{2+}, and its substitution onto a Co or Li site in $LiCoO_2$ is an aliovalent substitution that requires a mechanism for charge compensation. One possible mechanism is the formation of new electronic species. In this mechanism, the substitution of Mg^{2+} onto a Co^{3+} site leads to the extrinsic Mg_{Co} defect and a concomitant increase in the oxidation state of a Co site from 3+ to 4+, which introduces an impurity hole in the system. This mechanism was originally proposed to rationalize the high conductivity of Mg-doped $LiCoO_2$.[10,11] On the other hand, the substitution of Mg^{2+} onto a Li^+ site is balanced by the formation of a Co site with oxidation state +2, i.e an impurity electron is introduced in the system.

Other mechanisms for charge compensation can involve the formation of vacancy, interstitial and anti-site defects, and defect complexes.[44] In $LiCoO_2$, many intrinsic defects can combine with substitutional Mg and form a complex for charge compensation. Mg_{Co} can form a complex with electron donor defects such as V_O^+, Co_i^{2+}, Li_i and Co_{Li}^+, while Mg_{Li} with electron acceptor defects such as V_{Li}, V_{Co}^{2-}, Li_{Co}^-. Recent calculations[51,55] have shown that, of these ionic defects, the dominant one under typical synthesis conditions is the anti-site Co_{Li}^+ defect. The other intrinsic defects have high formation en-

ergies and are expected to have a low concentration.[51] Based on such reports, we considered in our initial calculations the Mg_{Co}-Co^{+}_{Li} complex as a charge compensation mechanism. However, the formation energy of this complex is over 1.5 eV when the system is under charge neutrality and, therefore, it was not further considered.[56] Instead, we considered the neutral complexes Mg_{Co}-Li_i and Mg_{Li}-V_{Li} as they can be relevant to the electrochemistry of Mg-doped $LiCoO_2$. Additionally, we studied the charge compensation by the dual substitution of Mg on Co and Li sites, i.e. the Mg_{Co}-Mg_{Li} complex.

To quantify the incorporation of Mg in $LiCoO_2$, we evaluated the formation energy of the possible extrinsic defects and defect complexes as:

$$E^f(X) = E_{tot}[X] - E_{tot}[LiCoO_2] - \sum_i n_i \mu_i \quad (1)$$

where X is a neutral extrinsic or intrinsic defect (or defect complex). $E_{tot}[X]$ and $E_{tot}[LiCoO_2]$ are the total energy of $LiCoO_2$ containing X and the total energy of the equivalent bulk $LiCoO_2$, respectively. n_i is the number of atomic species i added ($n_i > 0$) or removed ($n_i < 0$) from the supercell, while μ_i indicates the corresponding atomic chemical potentials. The stability of the complexes is quantified by their binding energies as:[57]

$$E_b = E^f(X) + E^f(Y) - E^f(XY) \quad (2)$$

where $E^f(XY)$, $E^f(X)$ and $E^f(Y)$ are the formation energy of the complexes and those of the individual defects, respectively. In this notation, a positive binding energy indicates a bound complex.

B. DFT Calculations

The total energies to evaluate Eq. (1) were calculated within the DFT framework as implemented on the Vienna Ab-initio Software Package (VASP).[58–61] We used the Perdew-Burke-Ernzerhof (PBE)[62,63] exchange and correlation functionals. The Li, O, Mg and Co ionic cores were represented by the projector augmented-wave (PAW) potentials[64,65] with 3, 6, 8 and 9 valence electrons, respectively. The wavefunction energy cutoff was set to 520 eV. We initialized the transition metal atoms in both high and low spin states with ferromagnetic ordering and the configuration with the lowest energy was used. The k-point mesh employed to calculate the bulk properties of $LiCoO_2$, CoO, Co_3O_4, Li_6CoO_4, Li_8CoO_6, Li_2O_2, Li_2O and MgO was 6×6×6, 8×8×8, 4×4×4, 4×4×4, 4×4×2, 6×6×6, 7×7×7, and 8×8×8, respectively. Gaussian broadening with an energy width of 0.1 eV was used for the Brillouin zone integration. These choices are sufficient to converge the bulk energies to better than 2 meV per primitive cell, which is substantially smaller than the variation due to the use of different functionals.

$LiCoO_2$ supercells with a defect X were calculated employing 4×4×2 supercells built from the primitive rhombohedral unit cell and 2×2×3 Monkhorst-Pack k-point meshes. The defects and defect complexes that were studied are shown schematically in Fig. 1. The extrinsic Mg defects were created by the substitution of a Co or Li atom in the $Li_{32}Co_{32}O_{64}$ supercell. The Li vacancy site was built by removing a Li from the supercell while the Li interstitial-site was constructed by adding a Li atom at the tetrahedral site in the Li layer. To simulate the Mg_{Co}-Li_i and Mg_{Li}-V_{Li} defect complexes in our supercell, we evaluated various configurations where the intrinsic Li defects were a first, second or third neighbors of the Mg site. These preliminary calculations indicated that the complexes are more stable when the Li defects are first neighbor to Mg. We found similar results for the Mg_{Co}-Mg_{Li} complex. Therefore, the extrinsic Mg defect is always a nearest neighbor of the second defect in the defect complexes that were studied. For each defect, all atomic positions were optimized until residual forces were less than 0.02 eV/Å. The volume of the supercell with the defects was fixed to that calculated for the primitive unit cell.

The use of supercells to study defects introduces quantum mechanical, elastic and electrostatic artifacts.[57] These artifacts become smaller as the supercell size is increased. In the present calculations, where we evaluated formation energies for neutral defects, only quantum mechanical (wavefunction overlap) and elastic effects are expected. We performed calculations with a larger 4×4×4 supercell to corroborate that the formation energies evaluated with a 4×4×2 supercell are relatively insensitive to these supercell size effects. For the substitution of Mg onto a Co site in $LiCoO_2$, the formation energy evaluated with the 4×4×2 supercell is 0.52 eV while with the 4×4×4 cell it is 0.55 eV. For the Mg_{Co}-Mg_{Li} complex, the formation energies calculated with the 4×4×2 and 4×4×4 supercells are 0.71 eV and 0.67 eV, respectively. We also evaluated the effect of volume relaxation for the substitution of Mg onto Co with the 4×4×2 supercell; the formation energy is 0.51 eV when volume relaxation is allowed, a 0.01eV difference from the fixed volume result.

The formation energies and electronic properties of metal-oxides are known to deviate from experimental results when evaluated with the generalized gradient approximation (GGA) to DFT.[52] Wang *et al.* have identified the overbinding of the O_2 molecule and the self-interaction of localized d-electrons in the transition metal as the main source of errors.[52] Various methods have been proposed to account for these errors.[49,52,53,67] One straightforward approach to correct the O_2 overbinding is to add an empirical correction.[52,67?] We have adopted this approach for all GGA-based calculations by adding a recently proposed[67] correction of +1.20 eV to the total energy of O_2. Our calculated dissociation energy of O_2

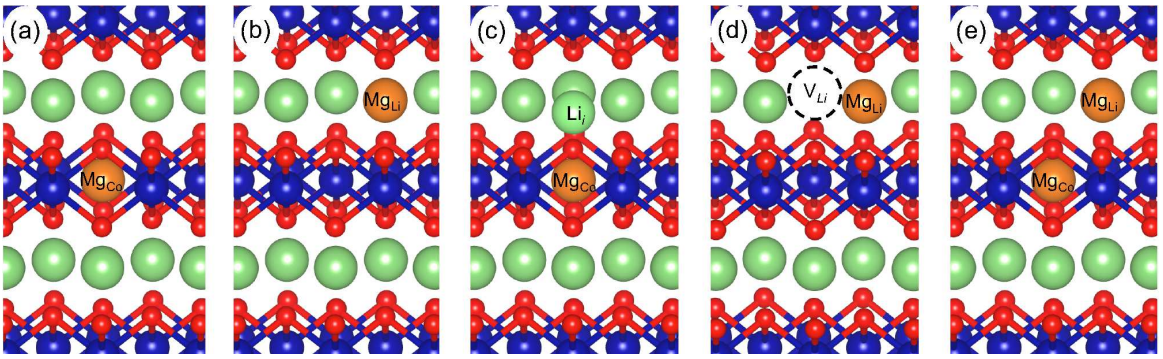

FIG. 1. Structures of Mg-doped $LiCoO_2$: a) Mg_{Co}, Mg on a Co site; b) Mg_{Li}, Mg on a Li site; c) Mg_{Co}-Li_i, complex of Mg_{Co} and a Li interstitial; d) Mg_{Li}-V_{Li}, complex of Mg_{Li} and a Li vacancy; and e) Mg_{Co}-Mg_{Li}, complex of Mg_{Co} and Mg_{Li}. Colored spheres indicate Mg (orange), Li (green), Co (blue), and O (red) atoms, respectively. Image generated with VESTA.[66]

is -4.85 eV after correction while the GGA uncorrected value is -6.05 eV; the corresponding experimental value is -5.13 eV.[69] The self-interaction error can be treated with an onsite Hubbard model correction.[47] We used the rotational invariant approach of Dudarev,[70] where a Coulomb parameter U and exchange parameter J are combined into a single U-J parameter. For simplicity, we hereafter refer to U instead of U-J. The electronic states and energetics calculated with this method can depend on the chosen value of U.[48,52] To study how the properties of Mg-doped $LiCoO_2$ changes with U, we performed calculations with U = 1.5, 3.3, 5.0, and 5.5 eV. We used the U parameter consistently for Co in all calculations, including metallic Co. Note that within this DFT+U and empirical correction scheme the energies of s and p orbitals are not directly affected, leaving the well known GGA binding energy errors[67,71,72] untreated except for the case of the O_2 molecule.

C. Chemical Potentials

To evaluate Eq. (1), we need to determine the atomic chemical potentials μ_i. The quaternary Li-Co-Mg-O phase diagram is available in the Materials Project[54,73,74] website.[75] From this phase diagram, one can expect separated Li-Co-O and MgO phases. Note that these are the known Li-Co-Mg-O phases but additional phases could exist. Based on this phase diagram, we approximate the atomic chemical potentials μ_i assuming that $LiCoO_2$ is stable and in contact with MgO.

The stability condition of $LiCoO_2$ requires that:

$$\Delta\mu_{Li} + \Delta\mu_{Co} + 2\Delta\mu_O = \Delta H^f\,(LiCoO_2) \qquad (3)$$

where ΔH^f is the formation enthalpy and $\Delta\mu_{Li} = \mu_{Li}^{LiCoO_2} - \mu_{Li}^{Li_{bulk}}$, $\Delta\mu_{Co} = \mu_{Co}^{LiCoO_2} - \mu_{Co}^{Co_{bulk}}$ and $\Delta\mu_O = \mu_O^{LiCoO_2} - \mu_O^{O_2(gas)}$. $\Delta\mu_i$ indicates[50,76,77] the possible variation of the chemical potential of atom i when $LiCoO_2$ is formed, where $\mu_i^{LiCoO_2}$ characterizes the chemical potential of atom i in $LiCoO_2$, and $\mu_i^{i_{bulk}}$ and $\mu_O^{O_2(gas)}$ the potential of atom i in bulk and an O atom in O_2. Absence of segregation of bulk Li, Co or formation of O_2 gas implies that $\Delta\mu_i \leq 0$. Additionally, $LiCoO_2$ competes with other possible Li-Co-O compounds, such as Li_2O, Li_2O_2, Li_8CoO_6, Li_6CoO_4, CoO and Co_3O_4.[49–51] Therefore, the chemical potentials are also constrained by:

$$x\Delta\mu_{Li} + y\Delta\mu_{Co} + z\Delta\mu_O \leq \Delta H^f\,(Li_xCo_yO_z) \qquad (4)$$

For MgO, the stability condition requires:

$$\Delta\mu_{Mg} + \Delta\mu_O = \Delta H^f\,(MgO) \qquad (5)$$

where $\Delta\mu_{Mg} = \mu_{Mg}^{MgO} - \mu_{Mg}^{Mg_{bulk}}$.

After accounting for all constraints, the range of Li and O chemical potentials that stabilize $LiCoO_2$ are defined in the ($\Delta\mu_{Li}$, $\Delta\mu_O$) plane. For a given point in this plane, $\mu_{Co}^{LiCoO_2}$ is determined from Eq. (3) and μ_{Mg}^{MgO} from Eq. (5).

III. RESULTS AND DISCUSSION

A. Range of Chemical Potentials

To determine the chemical potential range of Li and O that stabilize $LiCoO_2$, we evaluated ΔH^f of stable Li-Co-O compounds.[49–51] The results from GGA and GGA+U are given in Table I. The formation enthalpy of MgO and available experimental and previously calculated ΔH^f values are also included in Table I. Our calculated formation enthalpies are in general agreement with previous GGA and GGA+U calculations,[50–52] particularly for the non-transition metal-oxides and for GGA calculations. For the GGA+U results of Co-oxides some differences can be noticed. For instance, our calculated formation energy for $LiCoO_2$ with U = 3.3 and 5.0 eV is 0.7 - 0.8

TABLE I. Experimental[78,79] (at T = 298 K) and calculated formation enthalpy of Li-Co-O compounds and MgO in eV. Results from GGA (U = 0) and GGA+U calculations with U = 1.5, 2.4, 3.3, 5.0 and 5.5 eV are included. Previous GGA and GGA+U results are included for comparison. The enthalpies of MgO, Li_2O, and Li_2O_2 are U independent.

System	Exp.	U=0	U=1.5	U=2.4	U=3.3	U=5.0	U=5.5
$LiCoO_2$	-7.04	-7.10	-7.42	-7.61	-7.79, -7.12,[a] -7.13[c]	-7.77, -6.97[b]	-7.73
CoO	-2.46	-1.95, -1.9[d]	-2.44	-2.86	-3.31, -2.47,[a] -2.66[c]	-3.81, -3.8[b]	-3.94
Co_3O_4	-9.43	-9.36, -9.4[d]	-10.48	-11.23	-12.00, -9.76,[a] -9.92[c]	-12.41, -11.5[b]	-12.45
Li_6CoO_4		-20.66	-21.38	-21.82	-22.26, -21.54[c]	-22.74, -20.5[b]	-22.87
Li_8CoO_6		-29.39	-29.74	-29.94	-30.13, -29.50[c]	-30.14	-30.12
Li_2O_2	-6.56	-6.97, -7.04[a] -6.60[c]					
Li_2O	-6.21	-6.21, -6.2,[d] -6.28,[a] -5.5[b] -6.21,[c]					
MgO	-6.23	-6.04, -6.1[d] -6.14[c]					

[a] Ref. 50
[b] Ref. 51
[c] Ref. 54, 74, and 75
[d] Ref. 52

eV lower than the values in Refs. 50**?** , 51. The formation energy of CoO and Co_3O_4 evaluated with GGA+U also differs from Refs. 50**?** but resemble the results in Ref. 51. The source of the discrepancy between our results and Ref. 50 is unclear. The discrepancy with the results of Ref. 51 arises mainly because a correction factor for the O_2 overbinding was not used in that work.

We discuss first the deviation of our calculated formation enthalpies from the available experimental results to have an overall idea on the accuracy of the calculated chemical potentials. Note that the calculated formation enthalpies are at T= 0 K while the experimental results are at T = 298 K. However, the difference between 0 K and 298 K enthalpies is relatively small, within 0.1 eV per mol of O_2 for most transition metal-oxides.[52] Fig. 2 shows the deviation between calculated and experimental formation enthalpy. GGA reproduces the formation enthalpy of non-transition metal-oxides (Li_2O, Li_2O_2, and MgO) after correcting for the O_2 overbinding.[52,67] The error on the formation enthalpy of Li_2O and MgO is within 0.2 eV. For Li_2O_2, the error is 0.41 eV.

The formation enthalpy of Co-oxides evaluated within GGA are expected to deviate from experiment due to the self-interaction of localized *d*-electrons.[48,52] The deviation on the formation enthalpy of CoO evaluated with GGA is close to 0.50 eV. For $LiCoO_2$ and Co_3O_4, the corresponding deviation is relatively small, less than 0.1 eV. However, the oxidation energy of CoO ($6CoO + O_2 \rightarrow 2Co_3O_4$) is -7.04 eV, when evaluated with GGA, while the experimental value is -4.08 eV. GGA+U with U = 1.5 eV leads to a lower deviation of the formation enthalpy of CoO (0.03 eV) from experiment, but a greater deviation for $LiCoO_2$ (0.38 eV) and Co_3O_4 (1.19 eV).

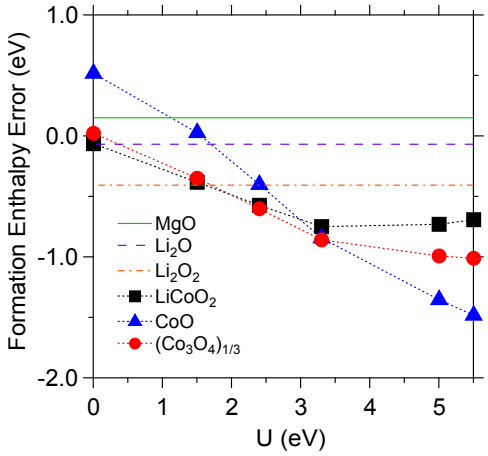

FIG. 2. Deviation between experimental and calculated formation enthalpies as function of U. Note that for the Co-oxides the error is per Co atom.

The oxidation energy of CoO is also large, -6.34 eV, a 2.26 eV error. The agreement with experiment for the oxidation of CoO is better when it is calculated with U = 3.3 eV;[52] the calculated oxidation energy is -4.15 eV, only an 0.07eV error. However, the error in the formation enthalpy of $LiCoO_2$, CoO and Co_3O_4 is above 0.70 eV when evaluated with U = 3.3 eV. As shown in Fig. 2, the agreement for the oxidation energy of CoO may be due to error cancelation because the error per Co atom of the formation energy of CoO and Co_3O_4 is the same for U = 3.3 eV. For U values over 3.3 eV, the formation enthalpies and relative energies of CoO and Co_3O_4 deviate

from experimental results by more than 1 eV.

The enthalpy of formation of $LiCoO_2$ is less sensitive to the U value than CoO and Co_3O_4. For U values from 3.3 to 5.5 eV, the deviation on the formation enthalpy of $LiCoO_2$ is centered on 0.7 eV. U values in this range are commonly used to study different processes and properties of $LiCoO_2$. U = 2.9 eV was used to study the electronic structure of $LiCoO_2$.[80] A U value of 3.3 eV has been used to study the phase diagram and surface properties of $LiCoO_2$.[50] This is also the value adopted for Co in the Materials Project.[?] This value of U was established from a fit to the experimental oxidation energy of CoO and the methodology of Wang *et al.*[52] to correct for the O_2 overbinding. U values close to 5.0 eV were used to calculate the average Li-intercalation potential,[48,71] and the defect chemistry[51] in $LiCoO_2$. U = 5.5 eV has been used to study the phase diagram and thermal decomposition of $LiCoO_2$.[49] U values close to 5.0 eV or 5.5 eV are taken from the self-consistently determined[48] U value of Co in layered $LiCoO_2$ or the average of U values of Co in different Co-oxides.

Clearly, the GGA+U method is limited in accuracy for relative energies of metal-oxides, even when empirically choosing U. This is not unexpected as the U parameter should be sensitive to the chemical environment of the atom sites where the correction is applied.[48] To calculate formation enthalpy of metal-oxides, the main problem is using the same U value to describe the atom sites in the metallic state (reactant) and the oxides (product). The method proposed by Jain *et al.*[53] and used in the Material Project is a possible solution to this problem. Formation enthalpies evaluated with this method are in reasonable agreement with experiments.[53] Yet, Jain's method relies on U values determined to describe formation enthalpies or oxidation energy of metal-oxides. This limits the usefulness of the method to study defects, as the U values are not necessarily transferable. As exemplified by $LiCoO_2$, a single U value cannot describe all properties, not even formation enthalpies and oxidation energies of the known parent phases of transition metal oxides to reasonable accuracy (< 0.5 eV).

We now discuss the phase stability diagram of $LiCoO_2$ and competing phases evaluated with GGA and GGA+U (Fig. 3). We have limited our analysis to the listed Li-Co-O compounds as these are the known or expected[49] thermally stable phases. For each diagram in Fig. 3, the colored polygon shows the range of O and Li chemical potentials that stabilize $LiCoO_2$. The reference for the chemical potential of O and Li is the O_2 molecule at 0 K and metallic lithium, respectively. The chemical potential of gaseous oxygen is dependent on temperature and partial pressure. One can approximate the chemical potential of gaseous oxygen assuming it to be an ideal gas on the basis of experimental data.[69] For instance, at ambient pressure and 1200 K, 900 K and 298 K, it is approximately 1.5, 1.0 and 0.3 eV below $\mu_O^{O_2(gas)}$.

Fig. 3(a) shows the chemical potential diagram constructed from available experimental formation enthalpy

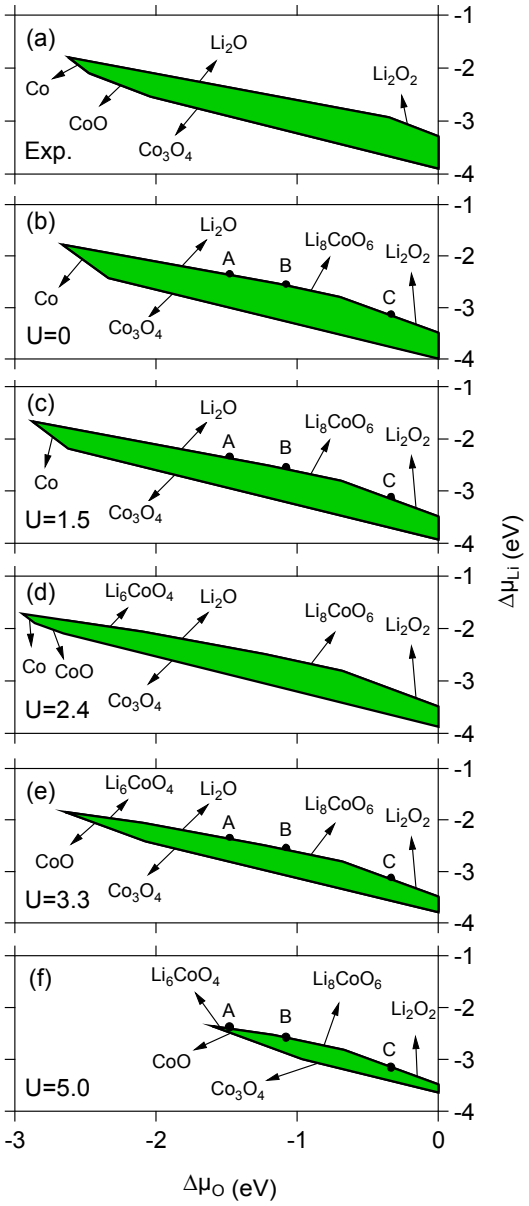

FIG. 3. Boundaries of the stable region of $LiCoO_2$ in the O and Li chemical potentials. The boundaries were constructed with the formation enthalpy from (a) experiment, (b) GGA and GGA+U with U values of (c) 1.5, (d) 2.4, (e) 3.3 and (f) 5.0 eV. The filled circles A, B, and C indicates the chemical potentials where defect formation energies were evaluated.

of Li-Co-O compounds at T = 298 K.[78,79] Fig. 3(b), (c), (d), (e) and (f) correspond to the phase diagrams from GGA and GGA+U calculations with U = 1.5, 2.4, 3.3 and 5.0 eV, respectively. All calculations predict a range of O and Li chemical potentials where $LiCoO_2$ is stable. Yet, the potential ranges differ from experiment and are noticeably sensitive to the U value. For instance, the maximum oxygen chemical potential where $LiCoO_2$ is stable change from -2.88 eV for calculations with U = 1.5 eV to only -1.60 eV for U = 5.0 eV. Moreover, only

calculations with U $\sim$ 2.4 eV reproduces all the phases that are in equilibrium with $LiCoO_2$. GGA and GGA+U with U = 1.5 eV predict the equilibrium between metallic Co and $LiCoO_2$ phases but not the equilibrium with the CoO phase (i.e. it is missing from the phase diagram). On the other hand, GGA+U with a U value of 3.3 eV or higher show the equilibrium of $LiCoO_2$ with CoO but not with metallic Co.

Based on these phase diagrams, we studied the extrinsic Mg defects in $LiCoO_2$ under three different chemical conditions, labeled as A, B and C. The chemical conditions A, B, and C corresponds to Li-rich condition at 0.2 atm oxygen and 1200 K, 900 K and 298 K, respectively. These conditions are indicated as filled circles in Fig. 3.

B. Defect Formation Energies

The electronic species formed upon the substitution of Mg on Co and Li sites can be in one of multiple spin configurations. To identify the configuration with the lowest energy, we examined various spin configurations for each defect. Similarly, spin configurations were evaluated for the Li_i and V_{Li} defects. The defect complexes of Mg have non-polarized spin configurations. The formation energy of Mg_{Co}, Mg_{Li}, Mg_{Co}-Li_i, Mg_{Li}-V_{Li} and Mg_{Co}-Mg_{Li} are shown in Fig. 4 as a function of U for a representative chemical condition. We also included the formation energy of Li_i and V_{Li}. The chemical condition correspond to point A in Fig. 3, representing the most Li-rich condition during synthesis at 1200 K.

As previously discussed, the formation of Mg_{Co} and Mg_{Li} leads to changes on the valency of Co atoms in $LiCoO_2$. As a result, the formation energy of these defects depends on the U value, Fig. 4(a). The change in the slope of the formation energy of Mg_{Co} and Mg_{Li} at U = 3.3 and 1.5 eV, respectively, corresponds to a transition from delocalized (low U) to localized (high U) states; see discussion in the next section. The same U dependence is also found in the formation energy of the V_{Li} and Li_i point defects since the valency of Co atoms also changes upon formation of these defects. The result for the formation energy of V_{Li} as function of U resembles previous calculations of the Li-insertion voltage in $LiCoO_2$.[48] In contrast to Mg_{Co} and Mg_{Li} defects, formation of the Mg defect complexes do not change the valency of Co in $LiCoO_2$ and their formation energies are rather insensitive to U, Fig. 4(b).

These results show the difficulty of studying Mg doping in $LiCoO_2$ employing GGA and GGA+U calculations. For instance, the preferred site location of Mg changes with the U value. Mg is preferentially located on Co sites for calculations with GGA and GGA+U with U below 5.0 eV, which is in line with experiments[11,12,15,22,25–31,81] showing that Mg is located at Co site. For calculations with U = 5.0 and 5.5 eV, however, Mg is equally stable on both Co and Li sites. Moreover, only GGA+U with U values around 1.5 eV predict the spontaneous formation

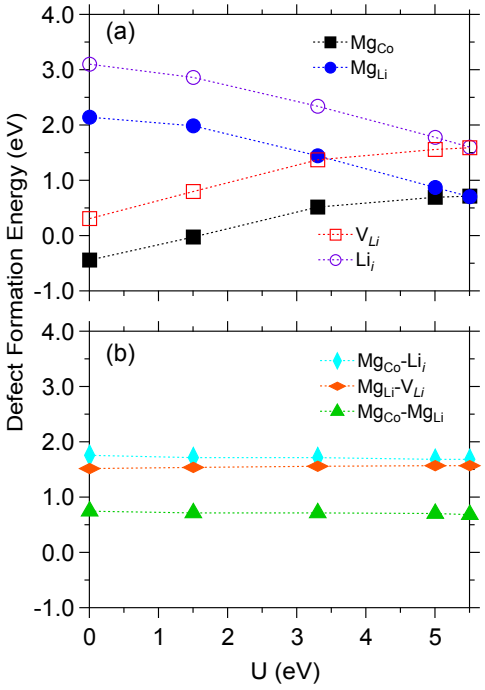

FIG. 4. Formation energy of (a) Mg and Li defects and (b) their complexes in $LiCoO_2$ as function of U. The energies are obtained at point A in the chemical potential diagram. Note overlapping symbols in (a) at the value U = 5.5.

of Mg-doped $LiCoO_2$. The formation energy of Mg_{Co} is -0.44 eV and -0.02 eV for GGA and GG+U with U = 1.5 eV, respectively. GGA+U calculations with U values of 3.3, 5.0 and 5.5 eV yield Mg_{Co} formation energies of 0.52, 0.70 and 0.72 eV, respectively, predicting that Mg will have a low solubility in $LiCoO_2$. However, Mg-doped $LiCoO_2$ with Mg/Co ratio as high as 0.5 have been synthesized,[26] demonstrating that this is not the case.

The formation energy of the Mg defects in $LiCoO_2$ depend on the atomic chemical potentials. We list in Table II the formation energy of Mg defects in $LiCoO_2$ for various chemical potentials. These potentials represent Li-rich environment and 0.2 atm O_2 at (A) 1200, (B) 900 and (C) 298 K. The formation energy of Mg_{Co} is reduced from point A to B and C while that of Mg_{Li} increases. Only GGA+U with U = 1.5 eV predicts Mg to be easily soluble in $LiCoO_2$ at points A, B and C. For greater U values, Mg_{Co} is energetically unfavorable at all points.

Table II also includes the formation and binding energy of the Mg_{Co}-Li_i, Mg_{Li}-V_{Li} and Mg_{Co}-Mg_{Li} complexes. The Mg_{Co}-Li_i and Mg_{Li}-V_{Li} complexes have high formation energies, from 1.1 to 2.2 eV at the various atomic chemical potentials and binding energy from 1.3 to 0.6 eV. The Mg_{Co}-Mg_{Li} complex has a formation energy close to 0.7 eV that is independent of the chemical potential and with binding energies from 0.7 to 1.3 eV. Although the formation energy of Mg_{Co}-Mg_{Li} is high, it is the lowest for U=5.5 eV at point A and often within

TABLE II. Calculated formation energy of Mg and Li defects and binding energy (BE) of their complexes in $LiCoO_2$ and in eV. Results from GGA (U = 0) and GGA+U calculations with U = 1.5, 3.3, 5.0 and 5.5 eV are included. The points A, B and C indicates the chemical potentials that were examined, corresponding to Li-rich condition and 0.2 atm O_2 at A: 1200 K, B: 900 K and C: 298 K.

	U=0				U=1.5				U=3.3				U=5				U=5.5			
Defects	A	B	C	BE	A	B	C	BE	A	B	C	BE	A	B	C	BE	A	B	C	BE
Mg_{Co}	-0.44	-0.64	-0.80		-0.02	-0.22	-0.38		0.52	0.32	0.16		0.70	0.50	0.34		0.72	0.52	0.36	
Mg_{Li}	2.15	2.34	2.50		1.99	2.19	2.35		1.45	1.66	1.82		0.88	1.08	1.24		0.71	0.91	1.07	
Li_i	3.10	3.30	3.88		2.86	3.06	3.64		2.34	2.54	3.12		1.78	1.98	2.57		1.60	1.80	2.38	
V_{Li}	0.31	0.11	-0.48		0.80	0.60	0.02		1.38	1.18	0.60		1.56	1.36	0.78		1.59	1.39	0.81	
Mg_{Co}-Li_i	1.76	1.76	2.18	0.90	1.72	1.72	2.14	1.12	1.72	1.72	2.14	1.14	1.69	1.69	2.11	0.79	1.69	1.69	2.11	0.63
Mg_{Li}-V_{Li}	1.52	1.52	1.10	0.92	1.54	1.54	1.12	1.24	1.56	1.56	1.14	1.28	1.57	1.57	1.14	0.88	1.57	1.57	1.14	0.73
Mg_{Co}-Mg_{Li}	0.75	0.75	0.75	0.95	0.72	0.72	0.72	1.24	0.72	0.72	0.72	1.25	0.71	0.71	0.71	0.87	0.69	0.69	0.69	0.74

a few 0.1 eV elsewhere. The formation energy of these complexes is insensitive to the U value and we can state with some certainty that these complexes are unlikely to form in Mg-doped $LiCoO_2$ due to their high formation energies.

C. Defect Geometries

To study the local geometry around Mg in $LiCoO_2$ as a function of U, we have tabulated in Table III the Mg-O and Co-O interatomic distances calculated with GGA and GGA+U. For the Mg_{Co} and Mg_{Li} defects, we also include the magnetic moment of the supercell and whether it is localized or delocalized. The localization was determined based on the local magnetic moments.

For Mg_{Co}, both GGA and GGA+U predict a low-spin configuration. Yet, for calculations with U = 3.3 or below, the state is delocalized while for U = 5.0 eV or above, it is localized. When the state is delocalized, the Mg-O distances are 2.04 Å independently of the U value (Table III). The Co-O distances of Co atoms nearest to Mg_{Co} are 1.94 Å, as in pristine $LiCoO_2$, when calculated with GGA. For GGA+U with U = 1.5 and 3.3 eV, these Co-O bonds are slightly distorted with distances of 1.94 and 1.93 Å. GGA+U results in a state that is delocalized mainly on the six Co atoms nearest to Mg_{Co} while GGA leads to a more delocalized state and undistorted Co-O bonds.

For the localized state predicted with U = 5.0 eV, the Mg-O bonds are distorted with distances ranging from 2.06 to 2.02 Å. A slightly higher U value, 5.5 eV, leads to higher distortion with Mg-O distances ranging from 2.07 to 1.95 Å. This distortion on the Mg-O bonds results from the formation of the localized holes on a Co atom near to Mg_{Co}. The Co-O bonds where the hole is located are also distorted with distances from 1.92 to 1.90 Å (Table III). Such bonds are shorter than 1.94 Å for Co-O in pristine $LiCoO_2$.

The impurity hole formed with Mg_{Co} in Mg-doped $LiCoO_2$ can be compared with other hole that can be formed in $LiCoO_2$. We performed calculations for the hole created with the formation of a Li vacancy; results are included in Table III. As for Mg_{Co}, both GGA and GGA+U predict a low-spin configuration, delocalized for calculations with U = 3.3 (or below) and localized for U = 5.0 eV (or above). Another hole is the one formed as an intrinsic electronic defect in pristine $LiCoO_2$. The formation of this state in $LiCoO_2$ was recently studied[51] with GGA+U (U = 5.0 eV) and methodologies similar to the present work. We therefore used this result for comparison. The intrinsic hole in $LiCoO_2$ was found to be localized with a low-spin configuration and Co-O distances of 1.91(×4) and 1.90(×2) Å.[51] The properties of this hole are similar to the one formed with Mg_{Co}; the main difference is the more distorted Co-O geometry in Mg-doped $LiCoO_2$.

For the impurity electron formed with the Mg_{Li} defect, GGA predicts a delocalized low-spin state. The Mg-O distances are all 2.08 Å while the Co-O bonds are distorted with interatomic distances from 1.96 to 1.93 Å. The Li-O interatomic distance in pristine $LiCoO_2$ is 2.11 Å. All calculations of the Mg_{Li} defect with GGA+U result on a localized high-spin configuration. In this case, the Mg-O bonds are distorted with distances ranging from 2.10 to 2.01 Å. The impurity electron is localized on a second nearest neighbor Co atom to Mg_{Li} with Co-O distances that range from 2.10 to 2.03 Å. These distances do not change significantly for calculations with the various U values.

The electron introduced with the Mg_{Li} defect is comparable to the electron introduced upon the formation of an interstitial Li atom in $LiCoO_2$. GGA predicts a delocalized low-spin state and GGA+U a delocalized high-spin state for Li_i as for the Mg_{Li} defect. The Co-O interatomic distances are also rather similar in both defects. For the electron as an intrinsic electronic defect in pristine $LiCoO_2$, Koyama *et al.*[51] found a localized low-spin state with Co-O distances of 2.06 (×6) Å.

In line with results for the formation energy, the characterization of the local geometry of defects that change the valency of Co atoms in $LiCoO_2$ is rather difficult with GGA+U calculations. The geometry of these defects is sensitive to the U value because increasing/decreasing U leads to localized/delocalized defect states (see discussion below). The situation is different for defect complexes. The geometry of the Mg defect complexes in $LiCoO_2$ does not depend on the U value. For all complexes the Mg-O and Co-O bonds are distorted with distances from 2.11 to 1.93 Å for Mg-O and from 1.95 to 1.92 Å for Co-O (Table III). For these type of defects that do not change the valency of Co, GGA+U calculations yield more con-

TABLE III. Total magnetic moment (MM per supercell in bohr magneton μ_B) and Mg-O and Co-O interatomic distances (Å) in Mg-doped $LiCoO_2$. Results are included for GGA and GGA+U calculations with U = 1.5, 3.3, 5.0 and 5.5 eV.

Defects	Property	U=0	U=1.5	U=3.3	U=5	U=5.5
Mg_{Co}	MM	1 - *delocalized*	1 - *delocalized*	1 - *delocalized*	1 - *localized*	1 - *localized*
	d(Mg-O)	2.04×6	2.04×6	2.04×6	2.06×2, 2.03×2, 2.02×2	2.07, 2.04, 2.03×2, 2.01, 1.95
	d(Co-O)	1.94×6	1.94×4, 1.93×2	1.94×4, 1.93×2	1.92×2, 1.91×2, 1.90×2	1.92×2, 1.91×2, 1.87×2
V_{Li}	MM	1 - *delocalized*	1 - *delocalized*	1 - *delocalized*	1 - *localized*	1 - *localized*
	d(Co-O)	1.95×2, 1.94×2, 1.92×2	1.94×2, 1.93×2, 1.92×2	1.94×2, 1.93×2, 1.92×2	1.92×2, 1.91×2, 1.89×2	1.92×2, 1.91×2, 1.89×2
Mg_{Li}	MM	1 - *delocalized*	3 - *localized*	3 - *localized*	3 - *localized*	3 - *localized*
	d(Mg-O)	2.08×6	2.09×2, 2.08×2 2.07, 2.01	2.10×2, 2.09, 2.08, 2.06×2	2.10×2, 2.09, 2.08, 2.06×2	2.10×2, 2.09, 2.08, 2.06×2
	d(Co-O)	1.96×2, 1.94×2, 1.93×2	2.08, 2.06×2, 2.05×3	2.10×2, 2.06, 2.05, 2.03×2	2.10×2, 2.06, 2.05, 2.04×2	2.10×2, 2.06, 2.05, 2.04×2
Li_i	MM	1 - *delocalized*	3 - *localized*	3 - *localized*	3 - *localized*	3 - *localized*
	d(Co-O)	1.98×2, 1.97, 1.92×2, 1.91	2.18×2, 2.14, 1.98, 1.97×2	2.16×2, 2.13, 2.00, 1.99, 1.98	2.14×3, 2.00×2, 1.98	2.15, 2.14, 2.13, 2.00, 1.99×2
Mg_{Co}-Li_i	d(Mg-O)	2.11×3, 1.98×3	2.11×3, 1.98×3	2.11×3, 1.98×3	2.11×3, 1.98×3	2.11×3, 1.98×3
	d(Co-O)	1.95, 1.94×2, 1.93×2, 1.92	1.94×3, 1.93×2, 1.92	1.94×3, 1.93×2, 1.92	1.94×3, 1.93×2, 1.92	1.94×3, 1.93×2, 1.92
Mg_{Li}-V_{Li}	d(Mg-O)	2.12×2, 2.08×2, 2.06×2	2.12×2, 2.08×2, 2.06×2	2.12×2, 2.08×2, 2.05×2	2.12×2, 2.08×2, 2.05×2	2.12×2, 2.08×2, 2.05×2
	d(Co-O)	1.95×2, 1.94×2, 1.92×2	1.95×2, 1.94×2, 1.92×2	1.95×2, 1.94×2, 1.92×2	1.95×2, 1.94×2, 1.92×2,	1.95×2, 1.94×2, 1.92×2
Mg_{Co}-Mg_{Li}	d(Mg_{Co}-O)	2.07×2, 2.04×2, 2.02×2	2.07×2, 2.04×2, 2.02×2	2.07×2, 2.04×2, 2.02×2	2.07×2, 2.04×2, 2.02×2	2.07×2, 2.04×2, 2.01×2
	d(Mg_{Li} -O)	2.10×2, 2.09, 2.08, 2.06×2	2.10×2, 2.09, 2.08, 2.06×2	2.10×2, 2.09, 2.08, 2.06×2	2.10×2, 2.09, 2.08, 2.06×2	2.10×2, 2.09, 2.08, 2.06×2

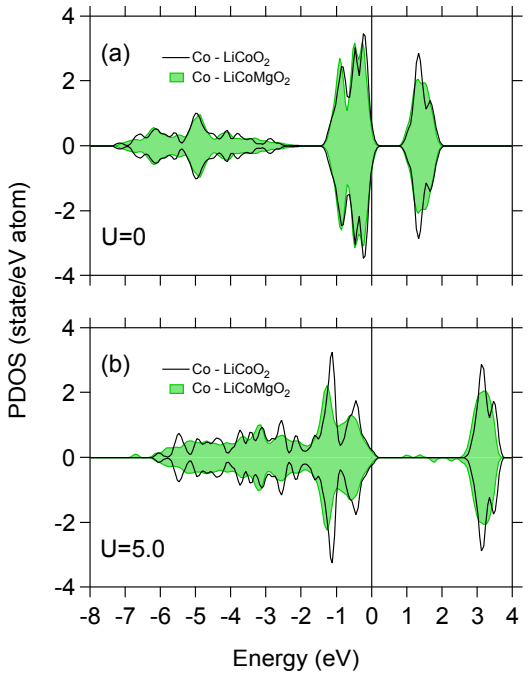

FIG. 5. Projected density of states (PDOS) of Co in $LiCoO_2$ (solid curve) and Mg-doped $LiCoO_2$ (green colored area). Panels (a) and (b) correspond to GGA and GGA+U (U = 5.0 eV) calculations of the Mg_{Co} extrinsic defect. The energy is relative to the Valence Band Maximum (VBM).

sistent geometric properties.

D. Electronic Structure

$LiCoO_2$ is a wide-band gap semiconductor. As found in previous calculations,[18,36,80,82–85] GGA underestimates the band gap from the Valence Band Maximum (VBM) to the Conduction Band Minimum (CBM), i.e. 0.94 eV. The experimental values are 2.1,[86] 2.5[87] and 2.7 eV.[88] For GGA+U calculations, the predicted band gap depends on the U value. The band gap calculated with U = 3.3 eV is 2.18 eV, in agreement with the experimental value of 2.1 eV in Ref. 86, while the value of U = 5.0 eV, 2.76 eV, reproduces the experimental value of 2.7 eV in Ref. 88. These GGA+U results are similar to previous calculations with U values close to 3[80] and 5 eV.[51,55,80,83,89]

The electronic structure of Mg-doped $LiCoO_2$ was studied by calculating the electronic band structure and density of states (DOS) with GGA and GGA+U. Fig. 5 displays the projected DOS (PDOS) of Co in $LiCoO_2$ and Mg-doped $LiCoO_2$. The PDOS of Co in Fig. 5(a) and (b) can be ascribed to three main groups.[90] The peaks from -7 to -2 eV corresponds to the occupied valence bands $e_g{}^b$, the group from -2 to 0.5 eV to the partially occupied valence band t_{2g} and the peaks from 0.5 to 4 eV to the unoccupied conduction band $e_g{}^*$.[90]

The PDOS of Co in Mg-doped $LiCoO_2$ calculated with GGA, Fig. 5(a), is rather similar to that in pristine $LiCoO_2$. Yet, some differences can be noticed. After Mg-doping, the PDOS in the energy range of the $e_g{}^b$ bands slightly increase while the PDOS in the region of the t_{2g} bands decrease. In the region of the $e_g{}^*$ bands, the PDOS also decrease. These changes in the electron distribution upon doping with Mg indicate that d-electrons move from nonbonding bands to bonding bands.[18] The result is a higher valence state for Co in Mg-doped $LiCoO_2$ than in $LiCoO_2$. In turn, the O anions become more closed-shell like as indicated by the decrease of the PDOS in $e_g{}^*$ bands region.[18] The electron distribution also changes if Mg is located on a Li site instead of Co (data not shown). Moreover, these changes are also observed on the PDOS of Co calculated with GGA+U , Fig. 5(b). Therefore, both GGA and GGA+U calculations suggest that the valence of Co in $LiCoO_2$ is modified when doping with

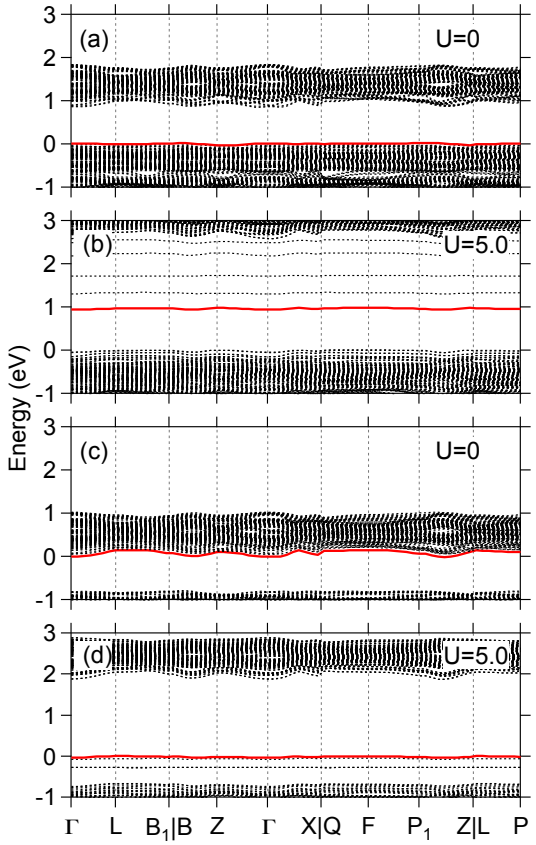

FIG. 6. Electronic band structures in the energy gap region of $LiCoO_2$ with the Mg_{Co} (a and b) and Mg_{Li} defect (c and d) calculated with (a and c) GGA and (b and d) GGA+U with U = 5.0. The solid red curve indicates the impurity band. The energy is relative to the Valence Band Maximum (VBM). The high-symmetry directions of the rhombohedral Brillouin zone were generated with AFLOW.[91]

Mg.

As discussed previously, Mg_{Co} in $LiCoO_2$ introduces an impurity hole in the system. This hole will be manifested in the band structure as an empty band close to the top of the valence band (shallow acceptor) or a band located "deep" in the band gap region. On the other hand, the formation of Mg_{Li} results in a electron that will lead to an occupied state close to the bottom of the conduction band (shallow donor) or an impurity state in the band gap region. In principle, both the shallow acceptor and shallow donor can increase the carrier density, leading to higher electronic conductivity. Conversely, no changes in electronic conductivity are expected if the impurity state is located in the band gap. Since Mg-doped $LiCoO_2$ have been shown[10,11] to have up to 2 orders of magnitude higher electronic conductivity than $LiCoO_2$, one can expect either shallow acceptor or donor states in the band structure of Mg-doped $LiCoO_2$.

The electronic band structure near the valence and conduction bands of $LiCoO_2$ with Mg_{Co} and Mg_{Li} is shown in Fig. 6. As expected, an empty band near the top of the valence band is predicted by GGA when Mg is located on Co, Fig. 6(a). Characteristic of a shallow acceptor level,[57] this level exhibits a similar dispersion as the upper valence band. A similar band structure is expected for GGA+U calculations with U = 1.5 and 3.3 eV since the geometry and spin-configuration of Mg_{Co} calculated with these methods are rather similar to those from GGA; this is confirmed by an increase in the density of states near the valence band maximum (data not shown). For GGA+U calculations with U = 5.0 eV or above, the impurity band associated with Mg_{Co} is located in the band gap region, Fig. 6(b). This level is spatially localized, leading to the local deformation observed for Co-O and Mg-O interatomic distances (Table III) and the splitting of unoccupied d-bands. When Mg is located on Li, calculation with GGA shows an occupied band near the conduction band, Fig. 6(c). Notice that this band is now positioned at the Fermi level (or VBM). This shallow donor level exhibits dispersion similar to the bottom conduction band. As in Mg_{Co}, GGA+U leads to a localized impurity band when Mg_{Li} is formed, Fig. 6(d).

The energy position of the impurity levels in Mg-doped $LiCoO_2$ are sensitive to the U value. For the Mg_{Co} defect, GGA and GGA+U calculations with U below 3.3 eV results on a shallow acceptor level, while calculations with U = 5.0 eV or higher leads to a localized level. The results of U = 3.3 eV or below explain the observed high electronic conductivity of Mg-doped $LiCoO_2$. However, these U values are not typically employed to study defects and impurities in $LiCoO_2$ or similar materials. Instead, self-consistently determined[48] U have been used.[45,51] For Co, the self-consistent U values range from 4.91 to 5.62 eV.[48] As our results show, U values in this range lead to deep levels in Mg-doped $LiCoO_2$, which is inconsistent with the observed high electronic conductivity of this material.

IV. CONCLUSIONS

In the present work, we have studied the doping of $LiCoO_2$ with Mg employing the GGA and GGA+U methods. In particular, we explored the effect of the U parameter on the energetic, geometric and electronic properties of Mg in $LiCoO_2$. Our results show that these properties for Mg located on a Co or a Li site in $LiCoO_2$ depend on the chosen U value. A similar dependence on U was also found in the properties of Li vacancy and Li interstitial defects in $LiCoO_2$. The similarity arises because the substitutional Mg and the Li defects lead to impurity states in $LiCoO_2$ with changes on the valency of Co in $LiCoO_2$. The strong dependence on U of the energetic, geometric and electronic properties is a direct consequence of the valency change of Co. Increasing the U value eventually changes the impurity states from shallow to deep levels. Conversely, if Mg on Co or Li sites forms complexes and no impurity states are introduced in $LiCoO_2$, the properties of such defect complexes are

insensitive to the U value.

These results indicate that GGA/GGA+U methods may be used to study isovalent substitution in $LiCoO_2$. For aliovalent substitution, such as Mg on a Co or a Li site, the usefulness of GGA/GGA+U methods is limited because experimental or theoretical data from accurate *ab initio* methods[3,4,92–94] are needed to validate the U dependent results. Moreover, even if such data were available, one is left with the problem of a single U value not giving a reasonable overall description of the properties of $LiCoO_2$. For example, U values close to 3[80] and 5[51,80,83,89] eV result in band gaps similar to experimental values, U = 3.3[50] eV correctly describes some of the major features in the phase diagram of $LiCoO_2$ while U values close to 5[48,71] eV are needed to reproduce the measured average Li-intercalation potential. Our present results show that U values of 3.3 eV and lower can describe the high electronic conductivity of Mg-doped $LiCoO_2$ but U as low as 1.5 eV are needed to describe the solubility of Mg in $LiCoO_2$. Finally, even if a perfect U value could be found, it would not improve the oxygen molecule formation energy or the thermodynamic properties of materials without d electrons. Empirical corrections would still be required.

ACKNOWLEDGMENTS

The work was supported by the Materials Sciences & Engineering Division of the Office of Basic Energy Sciences, U.S. Department of Energy (DOE). Research by PRCK was conducted at the Center for Nanophase Materials Sciences, which is sponsored at Oak Ridge National Laboratory by the Scientific User Facilities Division, Office of Basic Energy Sciences, U.S. Department of Energy.

[1] G. Ceder, G. Hautier, A. Jain, and S. Ong, MRS Bulletin **36**, 185 (2011).
[2] J. Kolorenč and L. Mitas, Rep. Prog. Phys. **74**, 026502 (2011).
[3] G. H. Booth, A. Grüneis, G. Kresse, and A. Alavi, Nature **493**, 365 (2013).
[4] L. Shulenburger and T. R. Mattsson, Phys. Rev. B **88**, 245117 (2013).
[5] "Materials genome initiative for global competitiveness," http://www.whitehouse.gov/mgi (2014).
[6] C. Wolverton and A. Zunger, Phys. Rev. Lett. **81**, 606 (1998).
[7] A. Van der Ven, M. K. Aydinol, G. Ceder, G. Kresse, and J. Hafner, Phys. Rev. B **58**, 2975 (1998).
[8] C. A. Marianetti, G. Kotliar, and G. Ceder, Nat. Mater. **3**, 627 (2004).
[9] J. P. Perdew and A. Zunger, Phys. Rev. B **23**, 5048 (1981).
[10] M. Carewska, S. Scaccia, F. Croce, S. Arumugam, Y. Wang, and S. Greenbaum, Solid State Ionics **93**, 227 (1997).
[11] H. Tukamoto and A. R. West, J. Electrochem. Soc. **144**, 3164 (1997).
[12] C. Julien, M. Camacho-Lopez, T. Mohan, S. Chitra, P. Kalyani, and S. Gopukumar, Solid State Ionics **135**, 241 (2000).
[13] M. Mladenov, R. Stoyanova, E. Zhecheva, and S. Vassilev, Electrochem. Commun. **3**, 410 (2001).
[14] R. Stoyanova, E. Zhecheva, M. I. Mladenov, P. Zlatilova, and S. Vassilev (Springer Netherlands, Dordrecht, 2002) pp. 463–468.
[15] S. Levasseur, M. Ménétrier, and C. Delmas, Chem. Mater. **14**, 3584 (2002).
[16] S. Madhavi, G. Subba Rao, B. Chowdari, and S. Li, Solid State Ionics **152153**, 199 (2002).
[17] G. Chen, C. Li, X. Xu, J. Li, and U. Kolb, Appl. Phys. Lett. **83**, 1142 (2003).
[18] X. G. Xu, C. Li, J. X. Li, U. Kolb, F. Wu, and G. Chen, J. Phys. Chem. B **107**, 11648 (2003).
[19] S. Frangini, S. Scaccia, and M. Carewska, Electrochim. Acta **48**, 3473 (2003).
[20] C. Li, X. Xu, C. Wang, Y. Xu, W. Xu, and G. Chen, J. Mater. Sci. Lett. **22**, 1183 (2003).
[21] P. Elumalai, H. Vasan, and N. Munichandraiah, J. Power Sources **125**, 77 (2004).
[22] H.-S. Kim, T.-K. Ko, B.-K. Na, W. I. Cho, and B. W. Chao, J. Power Sources **138**, 232 (2004).
[23] F. Nobili, S. Dsoke, F. Croce, and R. Marassi, Electrochim. Acta **50**, 2307 (2005).
[24] H. Xu, S. Xie, C. Zhang, and C. Chen, J. Power Sources **148**, 90 (2005).
[25] H.-J. Kim, Y. U. Jeong, J.-H. Lee, and J.-J. Kim, J. Power Sources **159**, 233 (2006).
[26] R. Sathiyamoorthi, P. Shakkthivel, R. Gangadharan, and T. Vasudevan, Ionics **13**, 25 (2007).
[27] J. Eom and J. Cho, J. Electrochem. Soc. **155**, A201 (2008).
[28] C. Zaheena, C. Nithya, R. Thirunakaran, A. Sivashanmugam, and S. Gopukumar, Electrochim. Acta **54**, 2877 (2009).
[29] F. Zhou, W. Luo, X. Zhao, and J. R. Dahn, J. Electrochem. Soc. **156**, A917 (2009).
[30] W. Luo, X. Li, and J. R. Dahn, J. Electrochem. Soc. **157**, A782 (2010).
[31] S. Valanarasu, R. Chandramohan, J. Thirumalai, T. A. Vijayan, S. R. Srikumar, and T. Mahalingam, J Mater Sci: Mater Electron **21**, 827 (2010).
[32] H.-G. Jung, N. V. Gopal, J. Prakash, D.-W. Kim, and Y.-K. Sun, Electrochim. Acta **68**, 153 (2012).
[33] F. Nobili, F. Croce, R. Tossici, I. Meschini, P. Reale, and R. Marassi, J. Power Sources **197**, 276 (2012).
[34] X. G. Xu, Y. J. Wei, X. Meng, C. Z. Wang, Z. F. Huang, and G. Chen, Acta Phys. Sin. **53**, 210 (2004).
[35] X. G. Xu, C. Z. Wang, W. Lu, X. Meng, Y. Sun, and G. Chen, Acta Phys. Sin. **54**, 313 (2005).
[36] S. Shi, C. Ouyang, M. Lei, and W. Tang, J. Power Sources **171**, 908 (2007).
[37] C.-C. Chang, J. Y. Kim, and P. N. Kumta, J. Electrochem. Soc. **147**, 1722 (2000).
[38] J. Cho, Chem. Mater. **12**, 3089 (2000).
[39] H.-J. Kweon, S. J. Kim, and D. G. Park, J. Power Sources **88**, 255 (2000).
[40] J. Cho, G. Kim, and H. S. Lim, J. Electrochem. Soc. **146**, 3571 (1999).
[41] C. Pouillerie, L. Croguennec, P. Biensan, P. Willmann, and C. Delmas, J. Electrochem. Soc. **147**, 2061 (2000).
[42] C. Pouillerie, F. Perton, P. Biensan, J. Prs, M. Broussely, and C. Delmas, J. Power Sources **96**, 293 (2001).
[43] A. D'Epifanio, F. Croce, F. Ronci, V. Rossi Albertini, E. Traversa, and B. Scrosati, Chem. Mater. **16**, 3559 (2004).
[44] J. Xiang, C. Chang, F. Zhang, and J. Sun, J. Electrochem. Soc. **155**, A520 (2008).
[45] K. Tatsumi, Y. Sasano, S. Muto, T. Yoshida, T. Sasaki, K. Horibuchi, Y. Takeuchi, and Y. Ukyo, Phys. Rev. B **78**, 045108 (2008).
[46] A. H. Tavakoli, H. Kondo, Y. Ukyo, and A. Navrotsky, J. Electrochem. Soc. **160**, A302 (2013).
[47] V. I. Anisimov, F. Aryasetiawan, and A. I. Lichtenstein, J. Phys.: Condens. Matter **9**, 767 (1997).
[48] F. Zhou, M. Cococcioni, C. A. Marianetti, D. Morgan, and G. Ceder, Phys. Rev. B **70**, 235121 (2004).
[49] L. Wang, T. Maxisch, and G. Ceder, Chem. Mater. **19**, 543 (2007).
[50] D. Kramer and G. Ceder, Chem. Mater. **21**, 3799 (2009).
[51] Y. Koyama, H. Arai, I. Tanaka, Y. Uchimoto, and Z. Ogumi,

Chem. Mater. **24**, 3886 (2012).
[52]L. Wang, T. Maxisch, and G. Ceder, Phys. Rev. B **73**, 195107 (2006).
[53]A. Jain, G. Hautier, S. P. Ong, C. J. Moore, C. C. Fischer, K. A. Persson, and G. Ceder, Phys. Rev. B **84**, 045115 (2011).
[54]A. Jain, S. P. Ong, G. Hautier, W. Chen, W. D. Richards, S. Dacek, S. Cholia, D. Gunter, D. Skinner, G. Ceder, and K. A. Persson, APL Materials **1**, 011002 (2013).
[55]K. Hoang and M. D. Johannes, J. Mater. Chem. A **2**, 5224 (2014).
[56]Calculations performed with GGA+U = 5.5 eV.
[57]C. G. Van de Walle and J. Neugebauer, J. Appl. Phys. **95**, 3851 (2004).
[58]G. Kresse and J. Hafner, Phys. Rev. B **47**, 558 (1993).
[59]G. Kresse and J. Hafner, Phys. Rev. B **49**, 14251 (1994).
[60]G. Kresse and J. Furthmüller, Comp. Mater. Sci. **6**, 15 (1996).
[61]G. Kresse and J. Furthmüller, Phys. Rev. B **54**, 11169 (1996).
[62]J. P. Perdew, K. Burke, and M. Ernzerhof, Phys. Rev. Lett. **77**, 3865 (1996).
[63]J. P. Perdew, K. Burke, and M. Ernzerhof, Phys. Rev. Lett. **78**, 1396 (1997).
[64]P. E. Blöchl, Phys. Rev. B **50**, 17953 (1994).
[65]G. Kresse and D. Joubert, Phys. Rev. B **59**, 1758 (1999).
[66]K. Momma and F. Izumi, J. Appl. Crystallogr. **41**, 653658 (2008).
[67]S. Grindy, B. Meredig, S. Kirklin, J. E. Saal, and C. Wolverton, Phys. Rev. B **87**, 075150 (2013).
[68]A. Jain, G. Hautier, C. J. Moore, S. Ping Ong, C. C. Fischer, T. Mueller, K. A. Persson, and G. Ceder, Comp. Mater. Sci. **50**, 2295 (2011).
[69]W. M. Haynes, *CRC Handbook of Chemistry and Physics, 94th edition* (Taylor & Francis Limited, 2013).
[70]S. L. Dudarev, G. A. Botton, S. Y. Savrasov, C. J. Humphreys, and A. P. Sutton, Phys. Rev. B **57**, 1505 (1998).
[71]V. L. Chevrier, S. P. Ong, R. Armiento, M. K. Y. Chan, and G. Ceder, Phys. Rev. B **82**, 075122 (2010).
[72]V. Stevanović, S. Lany, X. Zhang, and A. Zunger, Phys. Rev. B **85**, 115104 (2012).
[73]S. P. Ong, L. Wang, B. Kang, and G. Ceder, Chem. Mater. **20**, 1798 (2008).
[74]A. Jain, G. Hautier, S. Ong, C. Moore, C. Fischer, K. Persson, and G. Ceder, Phys. Rev. B **84**, 045115 (2011).
[75]https://materialsproject.org/#apps/phasediagram (2014).
[76]S.-H. Wei, Comp. Mater. Sci. **30**, 337 (2004).
[77]H. Dixit, N. Tandon, S. Cottenier, R. Saniz, D. Lamoen, and B. Partoens, Phys. Rev. B **87**, 174101 (2013).
[78]M. Wang and A. Navrotsky, J. Solid State Chem. **178**, 1230 (2005).
[79]M. W. Chase and National Institute of Standards and Technology (U.S.), (American Chemical Society ; American Institute of Physics for the National Institute of Standards and Technology, [Washington, D.C.]; Woodbury, N.Y., 1998).
[80]D. Ensling, A. Thissen, S. Laubach, P. C. Schmidt, and W. Jaegermann, Phys. Rev. B **82**, 195431 (2010).
[81]R. Thirunakaran, N. Kalaiselvi, P. Periasamy, and N. G. Renganathan, Ionics **9**, 388 (2003).
[82]M. T. Czyyk, R. Potze, and G. A. Sawatzky, Phys. Rev. B **46**, 3729 (1992).
[83]A. Juhin, F. de Groot, G. Vank, M. Calandra, and C. Brouder, Phys. Rev. B **81**, 115115 (2010).
[84]Z. H. Sun, W. H. Liu, Q. X. Wan, D. M. Li, and Z. H. Xiong, Adv. Mat. Res. **415-417**, 1643 (2011).
[85]T. Okumura, Y. Yamaguchi, M. Shikano, and H. Kobayashi, J. Mater. Chem. **22**, 17340 (2012).
[86]K. Kushida and K. Kuriyama, Solid State Commun. **123**, 349 (2002).
[87]J. Rosolen and F. Decker, J. Electroanal. Chem. **501**, 253 (2001).
[88]J. van Elp, J. L. Wieland, H. Eskes, P. Kuiper, G. A. Sawatzky, F. M. F. de Groot, and T. S. Turner, Phys. Rev. B **44**, 6090 (1991).
[89]F. Xiong, H. J. Yan, Y. Chen, B. Xu, J. X. Le, and C. Y. Ouyang, Int. J. Electrochem. Sci. **7**, 9390 (2012).
[90]M. K. Aydinol, A. F. Kohan, G. Ceder, K. Cho, and J. Joannopoulos, Phys. Rev. B **56**, 1354 (1997).
[91]W. Setyawan and S. Curtarolo, Comp. Mater. Sci. **49**, 299 (2010).
[92]L. K. Wagner, Int. J. Quantum Chem **114**, 94101 (2014).
[93]L. K. Wagner and P. Abbamonte, arXiv:1402.4680 [cond-mat] (2014).
[94]K. Foyevtsova, J. T. Krogel, J. Kim, P. R. C. Kent, E. Dagotto, and F. A. Reboredo, arXiv preprint arXiv:1402.5561 (2014).